Haptic Guidance Approach for the Alignment of Femur Fractures Using Robot-Assisted Surgical System*

Names

***Abstract* — Reducing femur fractures is a very tedious process and requires the manipulation of the femur segments in the 6-dimensional space. To mitigate these challenges, we aim to incorporate a haptic feedback approach that will guide the surgeons in aligning the femur segments while eliminating the challenges of unwanted manipulation and bone-bone collision. We developed a Bézier curve-based approach to generate virtual fixtures given the control points generated by an optimized A* path planning algorithm. The Bézier curve-based virtual fixture represents a guided path in the Robossis surgical robot 6-dimensional space, directing its end-effector through a sequence of desired poses while adhering to the optimized path provided by the A* algorithm. As the optimal path is determined, we provide a haptic-guided path to align the bone segments. The results show that the user, manipulating the haptic controller, was successfully able to align the femur fracture segments while adhering to the optimal path with a maximum deviation from the translation and rotation space of 3.0 (mm) and 1.5 (deg), respectively. As such, the result shows that the proposed method can provide an intuitive solution for surgeons to align femur fractures while eliminating the challenges of unwanted manipulation and bone-bone collision.**

I. Introduction

Reducing femur fractures is a challenging process and requires the accurate manipulation of the femur segments in the 6-dimensional space [1], [2]. Traditional manual surgical methods are limited due to the high instances of malalignments and damage to surrounding soft tissues, indicating the need for improved techniques [3], [4]. In response to these challenges, surgical robotics has emerged as a promising alternative, offering enhanced precision and control [1], [2]. Our team previously developed a surgical robotic system, referred to as the Robossis System (RS), Abedin-Nasab et al. [5], designed for the femur fracture surgical procedure. The RS has demonstrated potential to improve outcomes in benchtop and cadaveric experiments [6], [7], [8] however, advancements in its navigation are essential for further success. In this paper, we propose the Robossis system navigation method, which employs a haptic-guided approach to align femur fractures.

II. Related Work and Contribution

As surgical robotics become more integrated with modern healthcare, the integration of navigation and haptic feedback methods has become an apparent need to mitigate the risks and improve the outcome of surgical procedures [9], [10]. In addition, surgical robotic systems that use force feedback integrated into their control mechanisms are less erroneous in surgeries, leaving less collateral damage of soft tissue in contact with the surgical robot [11].

Furthermore, the Robossis Surgical Robot (RSR) is designed with high force and torque insertion capability [6], [7], [8] to meet the required traction forces of the muscle surrounding the femur; however, it places the patient at risk for unaccounted manipulation or bone-bone collision. So, we aim to mitigate these risks by developing a haptic virtual fixture-based method for aligning femur fractures.

The inclusion of virtual fixtures in the control of surgical robotics has significantly enhanced the precision, safety, and effectiveness of surgeries. These virtual fixtures are specifically engineered to improve the control and accuracy of surgical procedures. For example, Li et al. [12] developed an algorithm that would optimize guidance using the surgical tool being inserted inside the nasal cavity. Their research supports the notion that virtual fixtures increase control in robotic instruments, which can prevent unintended collisions made by the surgeon during ENT surgery, and hints at its potential in other operations. Another study determined that it would be more advantageous to use haptic virtual fixtures for manipulation in situations where fragile structures are present, comparing their use to other visual feedback methods such as a 2D monocular RGB camera and 3D voxel representation [13].

Other research also highlights that spatial motion constraints made by virtual fixtures show improvements in accuracy and task completion time [14]. Hong et al. supported this information with their research on haptic guidance and proposed that the guidance level can be adjusted during training sessions to match the skill level of the trainee [15]. Overall, the augmented reality that the virtual fixtures provide leads to a precise exchange with the surgical instrument. Ultimately, this allows surgeons to make better decisions and accurate movements, which is important during intense surgical procedures. This information supports the idea that a more strenuous task, like femur fracture reduction, can benefit from a virtual fixtures control approach.

In this work, we propose a novel Bézier curve-based haptic virtual fixture method to guide the surgeon(s) in aligning the bone segments. Specifically, we will guide the surgeon(s) to

*Research supported by ABC Foundation.

F. A. Author is with the National Institute of Standards and Technology, Boulder, CO 80305 USA (corresponding author to provide phone: 303-555-5555; fax: 303-555-5555; e-mail: author@ boulder.nist.gov).

S. B. Author, Jr., was with Rice University, Houston, TX 77005 USA. He is now with the Department of Physics, Colorado State University, Fort Collins, CO 80523 USA (e-mail: author@lamar. colostate.edu).

T. C. Author is with the Electrical Engineering Department, University of Colorado, Boulder, CO 80309 USA, on leave from the National Research Institute for Metals, Tsukuba, Japan (e-mail: author@nrim.go.jp).

align the bone segments while restricting them, via haptic feedback, to a predefined optimized path. This path must ensure minimal straining of the soft tissue while ensuring that the path taken is the shortest and that the bone segments do not collide.

III. Description of the Robossis system

The Robossis system is composed of a 7-DOF Haptic Controller (HC), referred to as the leader (Sigma.7, Force Dimension - Switzerland), and a 6-DOF Robossis Surgical Robot (RSR), referred to as the follower. The Sigma.7 HC is a hybrid robot structure based on a delta mechanism for 3-DOF translational movements, a serial mechanism for 3-DOF rotational movements, and a gripping component for 1-DOF [16], [17] (**Fig. 1**). Furthermore, the RSR employs a design with a three-armed parallel mechanism, with each arm is attached to a moving and fixed ring [5], [6] (**Fig. 1**). In our previous work, we demonstrated the kinematics of the leader-follower mechanisms and the control architecture that transfers the motion from the HC to the RSR [18]. In this work, we advance upon the RS by integrating a haptic virtual fixtures-based method for the alignment of femur segments.

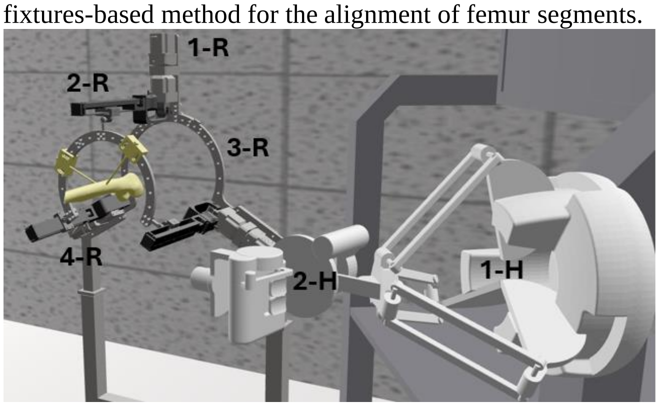

Figure 1. Representation of the Robossis leader-follower Robossis system. The HC consists of three identical legs connected in parallel (1-H), attaching between a top triangular fixed base and a mobile end-effector platform and coupled with a hybrid serial arm (2-H). The RSR consists of a moving ring (1-R), a fixed ring (2-R), and three arms, where each arm consists of a linear (3-R) and rotary actuator (4-R).

IV. Path Planning and Virtual Fixture Generation

A. 6-DOF State Space Search

According to the patient's CT images, 3D models of the fracture segments can be reconstructed to assess the extent of malrotation and malalignment. This enables the identification of the relative transformation between the proximal and distal bone segments that would achieve optimal alignment. We develop an optimized A* algorithm to determine the femur alignment path, leveraging its heuristic search capabilities. The A* algorithm is a heuristic search method characterized by its use of two primary functions: the cost function, denoted as ***G(n)***, and the heuristic function, denoted as ***H(n)***. Here, ***G(n)*** calculates the cost from the frontier node to any node n along the path, reflecting the distance to be traveled. Also, ***H(n)*** estimates the cost from the n node to the goal node, providing a forecast of the distance remaining. The A* algorithm combines these functions into an objective function guiding the search towards the goal by minimizing ***F(n)***. This approach systematically evaluates potential paths, prioritizing those with the lowest ***F(n)*** values, to efficiently determine an optimal route for distal bone segment realignment.

$$\boldsymbol{F(n) = G(n) + H(n)} \tag{1}$$

In the proposed method, we calculate ***H(n)*** using the Euclidean distance for translational and rotational spaces as

$$\boldsymbol{H}(\boldsymbol{n}) = \begin{bmatrix} \left\| \boldsymbol{X}_{\boldsymbol{goal,xyz}} - \boldsymbol{X}_{\boldsymbol{frontier,xyz}} \right\| \\ \left\| \boldsymbol{X}_{\boldsymbol{goal,\alpha\beta\gamma}} - \boldsymbol{X}_{\boldsymbol{frontier,\alpha\beta\gamma}} \right\| \end{bmatrix} \tag{2}$$

where $\boldsymbol{x}_{\boldsymbol{goal}} \in R^6$ is the final desired position and rotation of the bone segment attached to the RSR moving ring. Further, $\boldsymbol{x}_{\boldsymbol{frontier}} \in R^6$ is the potential n node location and rotation driven from the start node toward the goal node. Additionally, estimating the cost of the next potential n node position and rotation **G(n)** can be described as

$$\boldsymbol{G}(\boldsymbol{n}) = \begin{cases} \infty & \boldsymbol{if}\ \boldsymbol{P}_{\boldsymbol{x,y,z}} \cap \boldsymbol{D}_{\boldsymbol{x,y,z}} \\ \boldsymbol{g}(\boldsymbol{n}) & \boldsymbol{otherwise} \end{cases} \tag{3}$$

where $\boldsymbol{P}_{\boldsymbol{x,y,z}}$ and $\boldsymbol{D}_{\boldsymbol{x,y,z}}$ is the points cloud of the proximal and distal bone segments, respectively. For collision detection between bone segments, the distal bone segment, which is attached to the center of the moving ring of the RSR, is updated in real-time with respect to the potential n node position and orientation as

$$\boldsymbol{D}_{\boldsymbol{x,y,z}} = \boldsymbol{R}(\alpha, \beta, \gamma) * \boldsymbol{D}_{\boldsymbol{x,y,z,o}} + [x, y, z] \tag{4}$$

where $\boldsymbol{D}_{\boldsymbol{x,y,z,o}}$ is the original distal bone segment points cloud, $\boldsymbol{R}$ is the rotation matrix following Euler angles (x-y-z), $x, y, z \in \boldsymbol{X}_{\boldsymbol{frontier,xyz}}$ and $\alpha, \beta, \gamma \in \boldsymbol{X}_{\boldsymbol{frontier,\alpha\beta\gamma}}$. If there is an intersection between the proximal and distal bone segment, the cost of reaching that potential n node is expensive; therefore, an alternative node is explored.

Furthermore, $\boldsymbol{g}(\boldsymbol{n})$ is the cost from the frontier node to any node n along the path, reflecting the Euclidean distance to be traveled to the next frontier node. The state space search is explored by walking fixed steps in a grid-structure (1 mm and 1°) while prioritizing frontier nodes that minimize the objective function ***F(n).***

B. Virtual Fixture Generation

We implement the Bézier curve to generate virtual fixtures given the control points ($\boldsymbol{X}_{\boldsymbol{j}}^{A^*path} \in R^6$) generated via the A* algorithm. The Bézier curve-based virtual fixture represents a guided path in the RSR operational space, directing its end-effector through a sequence of desired poses while adhering to the optimized path provided by the A* algorithm. The equation for a Bézier curve is derived from the concept of Bernstein polynomials of degree n defined as

$$\boldsymbol{P}(\boldsymbol{t}) = \sum_{j=0}^{n} b_{j,n}\,(t)\,\boldsymbol{X}_{\boldsymbol{j}}^{A^*path} \tag{5}$$

where $\boldsymbol{P}(\boldsymbol{t}) \in R^6$ is the virtual fixtures on the Bézier curve, and $b_{j,\mathrm{n}}$ are the Bernstein polynomials of degree n. By using Bernstein polynomials, we ensure that the virtual fixtures $\boldsymbol{P}(\boldsymbol{t})$ will exhibit a smooth and continuous transition through the control points, which is essential for the force-guided path that should be free of abrupt movements or discontinuities.

C. Simulation and Analysis

We demonstrate the state space search for the realignment of the femur segments proposed in this work. We created a femur fracture as depicted in **Fig. 2 A,** where (1) and (2) show the proximal and distal bone segments, and (3) show the realigned distal bone segment. Further, **Fig. 2 A** (4) shows the explored and optimal locations to determine the optimal path for realignment of the femur segments. Further, comparative visualization of path planning in multiple spaces presented in **Fig. 2 (B), (C), & (D)**. Both the A* algorithm-generated path (red dots) and the Bézier curve-based virtual fixture (blue line with circles) are shown, where the Bézier curve smoothes and interpolates the discrete steps of the A* path into a continuous path to define the virtual fixtures.

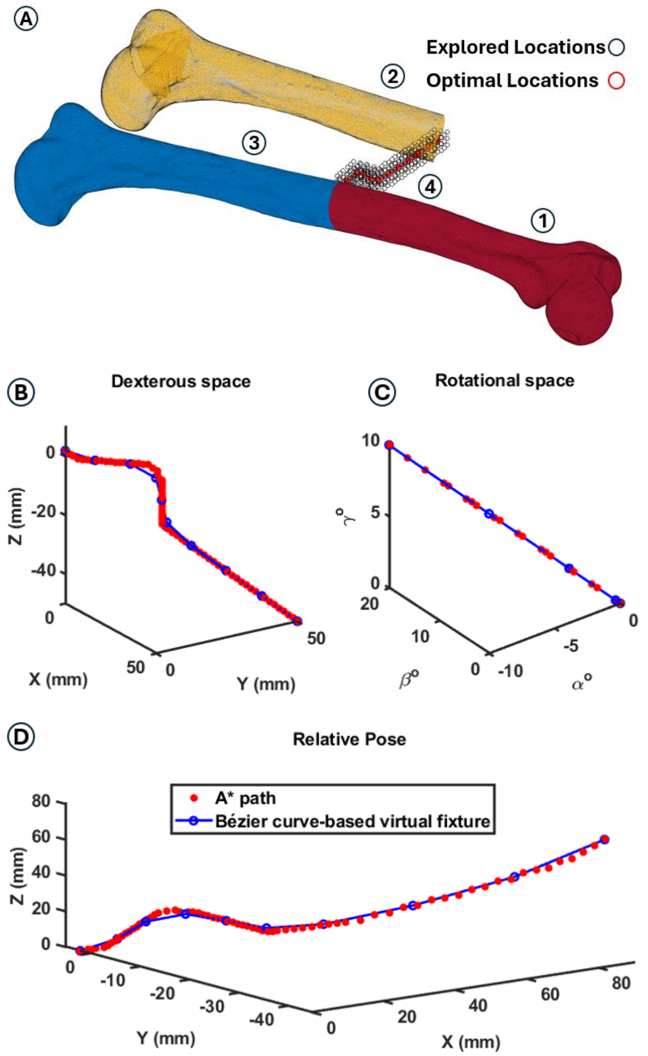

Figure 2. A) Demonstration of the state space search for the realignment of the femur segments. (1) and (2) shows the proximal and distal bone segments, (3) shows the realigned distal bone segment, and (4) presents the explored and optimal locations to determine the optimal path for realignment of the femur segments. Further, comparative visualization of path planning in multiple spaces: **B)** illustrates the trajectory in the dexterous space **C)** illustrates the rotational space **D)** merges these perspectives in the relative pose space, presenting a comprehensive view of the path and orientation. Both the A* algorithm-generated path (red dots) and the Bézier curve-based virtual fixture (blue line with circles) are shown, where the Bézier curve smoothes and interpolates the discrete steps of the A* path into a continuous path to define the virtual fixtures.

V. Force-Guided Algorithm

Once the optimal path is determined, the aim is to provide the surgeon(s) with a haptic-guided path to align the bone segments. Specifically, the surgeon manipulating the HC will be guided to moving only along the optimal path for bone alignment as defined via the virtual fixtures ($\boldsymbol{P} \in \boldsymbol{6}$).

A. Closest Pose to the Path

The virtual fixtures, which involve 3D poses, are decoupled into two distinct spaces: dexterous ($\boldsymbol{P}_{xyz} \in \mathrm{R}^3$) and rotation ($\boldsymbol{P}_{\alpha\beta\gamma} \in \mathbf{R}^3$). As such, the user hand 3D pose is decoupled into the dexterous ($\boldsymbol{x}_{HC}(\boldsymbol{t})_{xyz} \in R^3$) and rotation spaces ($\boldsymbol{x}_{HC}(\boldsymbol{t})_{\alpha\beta\gamma} \in R^3$). So, the closest pose can be determined by considering the application of vector projection (**Fig. 4**). Consider the vectors AB and AC, where AB extends from a specific virtual fixture $\boldsymbol{P}_{xyz,i}$ to the current hand position $\boldsymbol{x}_{HC}(\boldsymbol{t})_{xyz}$, and AC signifies the displacement from the current virtual fixture $\boldsymbol{P}_{xyz,i}$ to the subsequent fixture $\boldsymbol{P}_{xyz,i+1}$. The vectors AB and AC can be defined as:

$$\boldsymbol{AB} = \boldsymbol{x}_{HC}(\boldsymbol{t})_{xyz} - \boldsymbol{P}_{xyz,i} \tag{6}$$

$$\boldsymbol{AC} = \boldsymbol{P}_{xyz,i+1} - \boldsymbol{P}_{xyz,i} \tag{7}$$

where $i \in \{1,2,\dots,\mathrm{N}-1\}$ is an index within the virtual fixtures, with N being the index of the last fixture. To quantify the alignment of AB with AC, we compute the scalar projection length of AB onto AC, as

$$\mathrm{L} = \frac{\boldsymbol{AB} \cdot \boldsymbol{AC}}{|\boldsymbol{AC}|^2} \tag{8}$$

where L, representing the magnitude of AB projected in the direction of AC, and it is restricted to the interval [0, 1]. This constraint ensures that the projection of AB onto the path defined by AC remains within the physical confines of the virtual fixture path. As such, we can estimate the closest point on the dexterous path as:

$$\boldsymbol{S}_{xyz,i} = \boldsymbol{P}_{xyz,i} + \mathrm{L} * \boldsymbol{AC} \tag{9}$$

where $\boldsymbol{S}_{xyz}$ represents the point on the dexterous path connecting the i-th virtual fixture. Given the series of i-th virtual fixtures, we iterate through all segments defined by consecutive fixtures. For each segment, the scalar projection length L and the corresponding point $\boldsymbol{S}_{xyz}$ are computed. The iteration yields a set of potential points, from which the point $\boldsymbol{S}_{xyz}$ with the minimum deviation from the current hand position $\boldsymbol{x}_{HC}(\boldsymbol{t})_{xyz}$ is selected as the closest point on the dexterous path.

Furthermore, the closest point on the rotational path, denoted as $\boldsymbol{S}_{\alpha\beta\gamma}$, can be derived by leveraging the scalar projection length, L, which quantifies the extent to which the current hand position aligns with the direction of the virtual fixture path. This scalar L is used to interpolate between consecutive virtual fixtures to locate the point with the minimum deviation from the current hand rotation ($\boldsymbol{x}_{HC}(\boldsymbol{t})_{\alpha\beta\gamma}$). Thus, the closest point on the rotation path can be estimated as

$$\boldsymbol{S}_{\alpha\beta\gamma} = \boldsymbol{P}_{\alpha\beta\gamma,i} + \mathrm{L} * (\boldsymbol{P}_{\alpha\beta\gamma,i+1} - \boldsymbol{P}_{\alpha\beta\gamma,i}) \tag{10}$$

where $\boldsymbol{S}_{\alpha\beta\gamma}$ represents the point on the rotation path connecting the i-th virtual fixture. Algorithm 1 describes the method proposed to determine the closest pose ($\boldsymbol{S} \in \boldsymbol{R}^{\boldsymbol{6}}$) to the optimal path as defined by virtual fixtures ($\boldsymbol{P}$) given the pose of the user hand ($\boldsymbol{x_{HC}(t)}$) at time t.

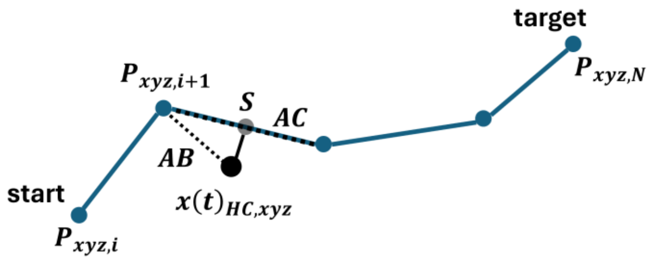

Figure 3. The method to determine the closest point to the translation path is demosntrated.

Algorithm 1: Closest Pose on Path

Input: $\boldsymbol{P} \in \boldsymbol{6}$ and $\boldsymbol{x_{HC}(t)} \in \boldsymbol{6}$, MinDist = inf;
For each index i from 1 to length($\boldsymbol{P}$) - 1
Compute Vectors:
$\boldsymbol{AB} \rightarrow \boldsymbol{Eq.6}$
$\boldsymbol{AC} \rightarrow \boldsymbol{Eq.7}$
Quantify the alignment of AB onto AC
$\boldsymbol{L} \rightarrow \boldsymbol{Eq.8}$ – clamp to interval [0, 1].
Closest point on the dexterous path
$\boldsymbol{S_{xyz,i}} \rightarrow \boldsymbol{Eq.9}$
Deviation from the user hand
DE = $\left\| \boldsymbol{S_{xyz}} - \boldsymbol{x_{HC}(t)_{xyz}} \right\|$
If DE < MinDist
MinDist = DE;
Closest point on the rotation path
$\boldsymbol{S_{\alpha\beta\gamma}} \rightarrow \boldsymbol{Eq.10}$
Out → Closest pose on path

B. *Haptic Feedback*

Each axis (translation and rotation) is modeled as a spring-damping system to provide the required haptic feedback to guide the user pose along the predefined optimal path. As the user pose ($\boldsymbol{x_{HC}(t)}$) deviate from the optimal path ($\boldsymbol{P}$), we determine the magnitude ($\|\boldsymbol{d}\| \in R^2$) and norm ($\widehat{\boldsymbol{n}} \in R^{2x3}$) of the deviation that would guide the user into the optimal path as

$$\|\boldsymbol{d}\| = \begin{bmatrix} \left\| \boldsymbol{S_{xyz}} - \boldsymbol{X_{HC}(t)_{xyz}} \right\| \\ \left\| \boldsymbol{S_{\alpha\beta\gamma}} - \boldsymbol{X_{HC}(t)_{\alpha\beta\gamma}} \right\| \end{bmatrix} \quad (11)$$

$$\widehat{\boldsymbol{n}} = \frac{\boldsymbol{d}}{\|\boldsymbol{d}\|}, \quad (12)$$

Further, we determine the haptic feedback projected in the user hand as

$$\boldsymbol{F} = -k_f * \|d\|_{xyz} * \widehat{\boldsymbol{n}}_{xyz} - c_f * \boldsymbol{v_{HC}} \quad (13)$$

$$\boldsymbol{\tau} = -k_\tau * \|d\|_{\alpha\beta\gamma} * \widehat{\boldsymbol{n}}_{\alpha\beta\gamma} - c_\tau * \boldsymbol{\omega_{HC}} \quad (14)$$

where $\boldsymbol{F} \in R^3$ and $\boldsymbol{\tau} \in R^3$ are the force and torque vectors applied at the specified locked axis, respectively. Also, c_f and c_τ are the damping constant (2 N s/m and 0.001 Nm s/deg); and k_f and k_τ are the spring constant (2000 N/m and 0.1 Nm/deg).

C. *Simulation and Analysis*

To demonstrate the haptic feedback magnitude along the fracture realignment path, we performed a simulation analysis. We create a 2D fracture scenario in the translational and rotational spaces, then we determine the optimal path as defined in section IV. We model the user pose ($\boldsymbol{x_{HC}(t)}$) as a fixed steps in a grid-structure and then we compute the haptic feedback in the translation ($\boldsymbol{F}$) and rotation ($\boldsymbol{T}$) spaces at each step. **Fig. 4** illustrates the results from the simulation analysis. As presented that as user pose deviate from the optimal path, as defined via the virtual fixtures, the haptic feedback increases as reaching maximum magnitude (15 N and 0.2 Nm). Whereas the user can move along the path with minimal force and torques projected on their hands. Also, the haptic feedback is modeled as a gradual haptic increase as the as user pose deviates from the optimal path.

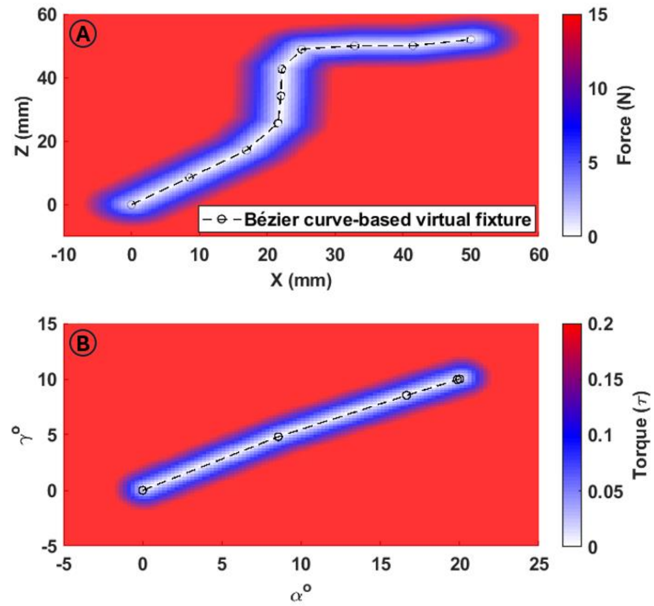

Figure 4. Simulation analysis to investigate the force and torque magnitude along the optimal path defined via the virtual fixture. As illustrated, as the user deviates from the optimal path, the haptic feedback increases gradually and reaches maximum magnitude (15 N and 0.2 Nm) for the translational **(A)** and rotational **(B)** space.

VI. Experimental Testing and Validation

A. *Robossis Surgical Simulator*

We use the Robossis Surgical Simulator (RSS), as developed in previous work [19], to create a midshaft femur fracture and validate the developed haptic guided algorithm for the fracture realignment. The RSS is an immersive environment that represent a realistic operating room for femur fracture surgery using the Robossis system, as previously completed in cadaver experiment (**Fig. 5 - A**). The RSS is designed to interact with the users using the HC Sigma-7 to manipulate the distal bone segment to the desired translational and rotational directions.

Also, as the user manipulates the HC, real-time visual rendering for the location of the bone is displayed as 2D fluoroscopic imaging via the Meta Quest headset. Also, the user has additional control via the Meta Quest controller, such as, the user is able to rotate the c-arm to the desired anatomical planar views, regulate each axis of the RSR, find the optimal path to align femur fracture, and able/disable the haptic guidance algorithm (**Fig. 5 - B**). Also, with the implementation of the HC, the user is prevented from overlapping the moving distal bone (attached to the RSR) with the proximal bone to recreate a realistic condition. Furthermore, the HC Sigma-7 end-effector global position and orientation trajectories, as commanded by the user's hand, are interfaced with the RSR as an incremental trajectory as

$$\boldsymbol{x(t)_{RSR}} = \boldsymbol{x_{RSR}(t-1)} + \boldsymbol{S} * (\boldsymbol{x(t)_{HC}} - \boldsymbol{x(t-1)_{HC}}) \quad (15)$$

where $\boldsymbol{x(t)_{RSR}} \in R^6$ and $\boldsymbol{x_{RSR}(t-1)} \in R^6$ are the current and previous location of the RSR, and $\boldsymbol{x(t)_{HC}} \in R^6$ and $\boldsymbol{x(t-1)_{HC}} \in R^6$ are the current and previous location of the HC (user's hands). Also, $\boldsymbol{S}$ is the scaling factor. We map the input of the user's hand-scaled trajectory's location and orientation ($\boldsymbol{x(t)_{RSR}}$) as the desired location of the Robossis end effector (center of the moving ring ($\boldsymbol{P}$)).

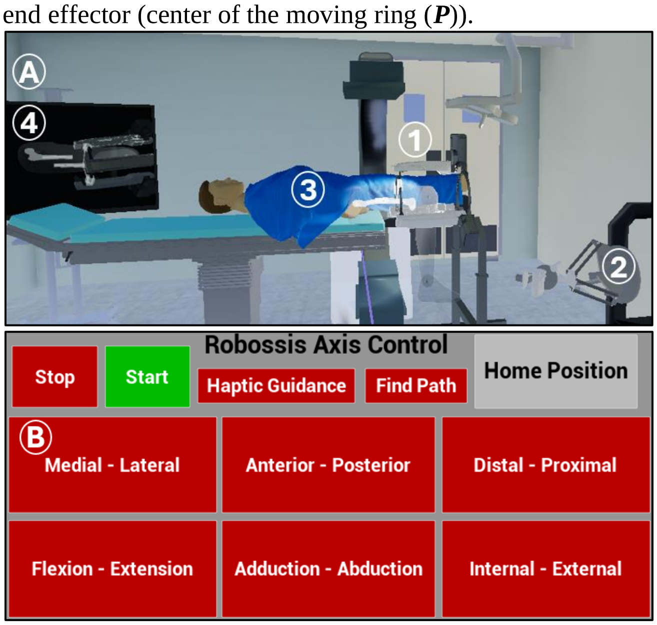

Figure 5. A) Demonstration of the Robossis Surgical Simulator (RSS) that is used to validate the developed haptic-guided algorithm for fracture realignment. The RSS was designed to include (1) the Robossis surgical robot, (2) the haptic controller, (3) a cadaver patient, a C-arm X-ray machine and (4) real-time visual rendering of the location of the bone is displayed as 2D fluoroscopic imaging. The environment was created with the goal to immerse the trained users in a similar operating room environment for femur fracture surgery using the Robossis system. **B)** The RSS Graphical User Interface (GUI) is illustrated. The GUI was designed to extend the usability and functionality of the RSS. Using the GUI, the user is able to regulate the motion of each axis (6 DOF), send the robot to the home position, find the path to align the fracture after varying maneuvers, and able/disable the haptic guidance algorithm to align the fractured femur.

B. *Midshaft Fracture Scenario and Realignment*

We created a realistic midshaft femur fracture (**Fig. 6 A**) where the fractured distal bone is translated to (-30 mm, 30 mm, 50 mm) and rotated (10°, 5°, 15°), in the world coordinate frame. Further, the proximal bone is located at (0 mm, 0 mm, 15 mm) and rotated (0°, 0°, 0°), in the world coordinate frame. With the presented scenario, the goal is to determine the optimal poses to align the proximal and distal bone segments while avoiding collisions (**Fig. 6 B**). **Fig. 6 C & D** illustrate the translational and rotational motion from the user (left) and the Bézier curve-based virtual fixture path (right). As shown that the user interacting with the haptic controller is guided to follow the Bézier curve-based virtual fixture path for the translation and rotational spaces, consecutively. As such, the distal bone segment, which is connected to the RSR moving ring, is directed through a sequence of desired poses while adhering to the optimized path. **Fig . 6 E** illustrates the haptic feedback that is projected into the user hand, via the haptic controller, to keep the motion of the user into the optimal path. Further, the results show that the user, manipulating the haptic controller, was successfully able to align the femur fracture segments while adhering to the optimal path with a maximum deviation from the translation and rotation space of 3.0 (mm) and 1.5 (deg), respectively (**Fig 6. F**).

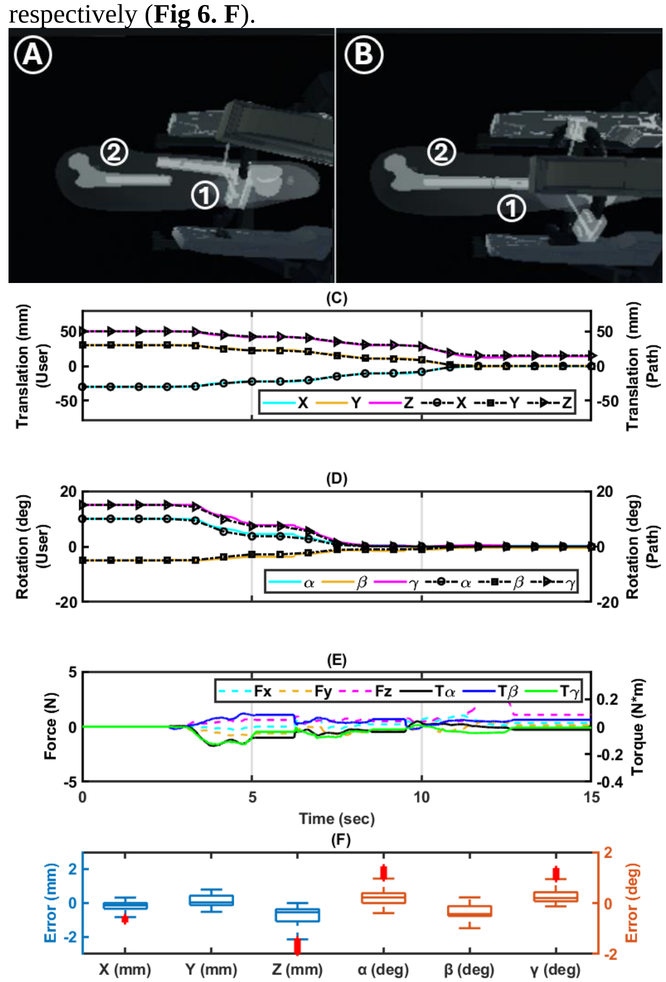

Figure 6. Demonstration of the midshaft femur fracture experimental case. **A)** shows the 2D fluoroscopic imaging of the fractured femur bone, and the Robossis surgical robot. **B)** shows the aligned femur bone after realignment procedure. **C & D)** illustrate the translational and rotational motion from the user (left) and the Bézier curve-based virtual fixture path (right). As shown the user interacting with the haptic controller is guided to follow the Bézier curve-based virtual fixture path for the translation and rotational spaces, consecutively. **E)** illustrates the haptic feedback that is projected into the user hand, via the haptic controller, to keep the motion of the user into the optimal path. **F)** The results show that the user, manipulating the haptic controller, was successfully able to align the femur fracture segments while adhering to the optimal path with a maximum deviation from the translation and rotation space of 3.0 (mm) and 1.5 (deg), respectively.

VII. Discussion

In this work, we proposed a novel Bézier curve-based haptic virtual fixture method to guide the surgeon(s) in aligning the bone segments. This method is specifically designed to provide navigational aid to surgeons during the process of aligning fractured femur segments. By integrating this approach, we aim to enhance precision and control in the surgical procedures, thereby addressing common challenges associated with previous methods.

A key innovation of our method is the incorporation of the modified A* algorithm in generating virtual fixtures. This approach helps create smooth, continuous paths, enabling surgeons to adhere to the optimal trajectory with haptic feedback. The incorporation of haptic feedback is essential as it introduces a sense of resistance when the surgeon deviates from the intended path, thus ensuring more precise and accurate alignment of bone segments. Further, another innovation of our work is the proposed method of determining the closest pose along the Bézier curve-based virtual fixture to the user hand pose. This allow for the accurate estimation of the haptic feedback to be projected onto user hand.

The results from the simulation study highlight the clear benefits of utilizing our Bézier curve-based approach. Notably, our strategy diminishes unnecessary movements that often result from incorrect handling or misalignment, leading to safer surgical environments. Additionally, our method promotes a structured and guided surgical process, which significantly enhances surgical performance. This improvement is seen in the increased efficiency and precision with which surgeons can complete their tasks, thereby revolutionizing standard practices.

For future, we plan to extend our research by developing a lower extremity muscle model based on the Hill-based Model. This development aims to refine our path planning algorithm, optimizing it to follow a trajectory that ensures optimal force application and torque distribution on the surgical robot, thereby improving the overall surgical outcome and patient recovery. Also, we aim to test this in cadaveric experiment to demonstrate the visibility, advantages of the proposed method.

VIII. CONCLUSION

Our works develop a novel approach to navigation through the use of Bézier curve-based haptic virtual fixtures, integrated with the A* algorithm for virtual fixture generation. This innovative method provides significant advancements in the field of robotic surgery, particularly in the precise alignment of bone segments. By offering surgeons a guided and controlled environment through haptic feedback, our approach minimizes the risk of errors associated with manual techniques, thereby enhancing surgical safety and efficiency.

IX. REFERENCES

[1] J. X. Zhao, C. Li, H. Ren, M. Hao, L. C. Zhang, and P. F. Tang, “Evolution and Current Applications of Robot-Assisted Fracture Reduction: A Comprehensive Review,” *Annals of Biomedical Engineering*, vol. 48, no. 1. Springer, pp. 203–224, Jan. 01, 2020. doi: 10.1007/s10439-019-02332-y

[2] L. Bai, J. Yang, X. Chen, Y. Sun, and X. Li, “Medical robotics in bone fracture reduction surgery: A review,” *Sensors (Switzerland)*, vol. 19, no. 16, Aug. 2019, doi: 10.3390/s19163593

[3] M. Citak *et al.*, “Femoral malrotation following intramedullary nailing in bilateral femoral shaft fractures,” *Arch Orthop Trauma Surg*, vol. 131, no. 6, pp. 823–827, Jun. 2011, doi: 10.1007/s00402-010-1245-6

[4] C. Zeckey *et al.*, “Femoral malrotation after surgical treatment of femoral shaft fractures in children: a retrospective CT-based analysis,” *European Journal of Orthopaedic Surgery and Traumatology*, vol. 27, no. 8, pp. 1157–1162, Dec. 2017, doi: 10.1007/s00590-017-1978-9

[5] M. H. Abedinnasab, F. Farahmand, B. Tarvirdizadeh, H. Zohoor, and J. Gallardo-Alvarado, “Kinematic effects of number of legs in 6-DOF UPS parallel mechanisms,” *Robotica*, vol. 35, no. 12, pp. 2257–2277, 2017, doi: 10.1017/S0263574716000862

[6] M. S. Saeedi-Hosseiny, F. Alruwaili, S. McMillan, I. Iordachita, and M. H. Abedin-Nasab, “A Surgical Robotic System for Long-Bone Fracture Alignment: Prototyping and Cadaver Study,” *IEEE Trans Med Robot Bionics*, vol. 4, no. 1, pp. 172–182, Feb. 2022, doi: 10.1109/TMRB.2021.3129277

[7] F. Alruwaili, M. S. Saeedi-Hosseiny, M. Clancy, S. McMillan, I. I. Iordachita, and M. H. Abedin-Nasab, “Experimental Evaluation of a 3-Armed 6-DOF Parallel Robot for Femur Fracture Surgery,” *J Med Robot Res*, vol. 07, no. 04, p. 2241009, Feb. 2022, doi: 10.1142/s2424905x22410094. Available: https://app.dimensions.ai/details/publication/pub.1152285333

[8] M. S. Saeedi-Hosseiny *et al.*, “Automatic Alignment of Fractured Femur: Integration of Robot and Optical Tracking System,” *IEEE Robot Autom Lett*, 2023.

[9] M. Kurt Pehlivanoğlu *et al.*, “A new surgical path planning framework for neurosurgery,” *The International Journal of Medical Robotics and Computer Assisted Surgery*, vol. 20, no. 1, p. e2576, 2024.

[10] Y. Chen, M.-Z. Pan, Z. Li, Y.-W. Deng, X.-L. Liao, and G.-B. Bian, “Autonomous path planning with muscle force optimization for robot assisted pelvic fracture closed reduction,” *IEEE Trans Med Robot Bionics*, 2023.

[11] C. R. Wagner, N. Stylopoulos, and R. D. Howe, “Presented at the Tenth Symposium on Haptic Interfaces for Virtual Environment and Teleoperator Systems The Role Of Force Feedback In Surgery: Analysis Of Blunt Dissection.”

[12] M. Li and R. H. Taylor, “Optimum robot control for 3D virtual fixture in constrained ENT surgery,” in *Medical Image Computing and Computer-Assisted Intervention-MICCAI 2003: 6th International Conference, Montréal, Canada, November 15-18, 2003. Proceedings 6*, Springer, 2003, pp. 165–172.

[13] K. Huang, D. Chitrakar, F. Rydén, and H. J. Chizeck, “Evaluation of haptic guidance virtual fixtures and 3D visualization methods in telemanipulation—a user study,” *Intell Serv Robot*, vol. 12, no. 4, pp. 289–301, 2019.

[14] M. Li and R. H. Taylor, “Performance of surgical robots with automatically generated spatial virtual fixtures,” in *Proceedings of the 2005 IEEE International Conference on Robotics and Automation*, IEEE, 2005, pp. 217–222.

[15] M. Hong and J. W. Rozenblit, “A haptic guidance system for computer-assisted surgical training using virtual fixtures,” in *2016 IEEE International conference on systems, man, and cybernetics (SMC)*, IEEE, 2016, pp. 2230–2235.

[16] A. Tobergte and P. Helmer, “A disturbance observer for the sigma. 7 haptic device,” in *2013 IEEE/RSJ International Conference on Intelligent Robots and Systems*, IEEE, 2013, pp. 4964–4969.

[17] A. Tobergte *et al.*, “The sigma. 7 haptic interface for MiroSurge: A new bi-manual surgical console,” in *2011 IEEE/RSJ International Conference on Intelligent Robots and Systems*, IEEE, 2011, pp. 3023–3030.

[18] F. H. Alruwaili *et al.*, “Design and Experimental Evaluation of a Haptic Robot-Assisted System for Femur Fracture Surgery,” *arXiv preprint arXiv:2310.19153*, 2023.

[19] F. H. Alruwaili *et al.*, “Haptic-Enhanced Virtual Reality Simulator for Robot-Assisted Femur Fracture Surgery,” *arXiv preprint arXiv:2310.19187*, 2023.